Neurobiology of Disease 201 (2024) 106665

Contents lists available at ScienceDirect

Neurobiology of Disease

journal homepage: www.elsevier.com/locate/ynbdi

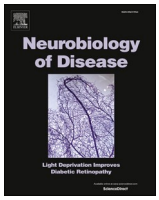

The proteomic signature of circulating extracellular vesicles following intracerebral hemorrhage: Novel insights into mechanisms underlying recovery

Laura Casado-Fernández [a,1], Fernando Laso-García [a,1], Dolores Piniella [a,b], Mari Carmen Gómez-de Frutos [a,c,d], Laura Otero-Ortega [a], Susana-Belén Bravo [e], Blanca Fuentes-Gimeno [a], Félix Docando [f], Elisa Alonso-López [a], Gerardo Ruiz-Ares [a], Jorge Rodríguez-Pardo [a], Ricardo Rigual [a], Elena de Celis-Ruiz [a], Carlos Hervás [a], Exuperio Díez-Tejedor [a], María Gutiérrez-Fernández [a,2,*], María Alonso de Leciñana [a,2,*]

[a] Neurological Sciences and Cerebrovascular Research Laboratory, Department of Neurology and Stroke Center, Neurology and Cerebrovascular Disease Group, Neuroscience Area Hospital La Paz Institute for Health Research - IdiPAZ (La Paz University Hospital – Universidad Autónoma de Madrid), Madrid, Spain
[b] Faculty of Medicine, Universidad Alfonso X el Sabio, Villanueva de la Cañada, Madrid, Spain
[c] Faculty of Health Sciences - HM Hospitals, University Camilo José Cela. Villanueva de la Cañada, Madrid, España
[d] Instituto de Investigación Sanitaria HM Hospitales, 28015 Madrid, Spain
[e] Proteomic Unit, Health Research Institute of Santiago de Compostela (IDIS), Santiago de Compostela, Spain
[f] Electron Microscopy Unit, Scientific-Technical Central Units, Institute of Health Carlos III (ISCIII), 28220 Majadahonda, Madrid, Spain

ARTICLE INFO

Keywords:
Intracerebral hemorrhage
Extracellular vesicles
Proteomics
Pathophysiology

ABSTRACT

Circulating extracellular vesicles (EVs) can participate in innate repair processes triggered after intracerebral hemorrhage (ICH). We aimed to describe changes in the proteomic profile of circulating EVs between the acute and subacute phases of ICH and to compare the findings depending on outcomes, as an approach to unraveling such repair mechanisms.

This was a prospective observational study including patients with non-traumatic supratentorial ICH. Exclusion criteria were previous disability, signs of herniation on baseline computed tomography, or limited life expectancy. EVs were isolated from blood samples at 24 h and 7 days after symptom onset. After 6-months' follow-up, patients were dichotomized into poor and good outcomes, defining good as an improvement of >10 points or > 50 % on the National Institutes of Health Stroke Scale and a modified Rankin Scale of 0–2. The protein cargo was analyzed by quantitative mass spectrometry and compared according to outcomes.

Forty-four patients completed follow-up, 16 (35.5 %) having good outcomes. We identified 1321 proteins in EVs, 37 with differential abundance. In patients with good outcomes, proteins related to stress response (DERA, VNN2, TOMM34) and angiogenesis (RHG01) had increased abundance at 7 days. EVs from patients with poor outcomes showed higher levels of acute-phase reactants (CRP, SAA2) at 7 days compared with 24 h.

In conclusion, the protein content of circulating EVs in patients with ICH changes over time, the changes varying depending on the clinical outcome, with greater abundance of proteins potentially involved in the repair processes of patients with good outcomes.

* Corresponding author at: Neurological Sciences and Cerebrovascular Research Laboratory, Department of Neurology and Stroke Center, Paseo de la Castellana, 261, 28046 Madrid, Spain.
E-mail addresses: mgutierrezfernandez@salud.madrid.org (M. Gutiérrez-Fernández), malecinanacases@salud.madrid.org (M. Alonso de Leciñana).
[1] These authors share first authorship.
[2] These authors are co-leads for this work.

https://doi.org/10.1016/j.nbd.2024.106665
Received 24 March 2024; Received in revised form 19 May 2024; Accepted 11 September 2024
Available online 12 September 2024

1. Introduction

Intracerebral hemorrhage (ICH) is a severe form of stroke that has no specific treatment clearly demonstrating efficacy in improving outcomes. Current therapy is based on supportive care, management of increased intracranial pressure, control of blood pressure, and reversal of anticoagulation when applicable. These measures can be lifesaving and might help prevent hematoma expansion in the hyperacute phase; however, they cannot reverse the damage caused by bleeding (Greenberg et al., 2022; Sandset et al., 2021).

The mechanisms underlying ICH-induced brain injury and their timelines limit the window of opportunity for some therapeutic approaches. Bleeding into the brain causes primary damage as soon as it occurs and is related to physical disruption of brain tissue, mass effect, and the toxic effect of blood products leaked into the parenchyma (Shao et al., 2019; Magid-Bernstein et al., 2022). This is followed by secondary biochemical and inflammatory cascades triggered by the blood products and molecular components released from damaged brain cells, culminating in further tissue damage (Magid-Bernstein et al., 2022).

Simultaneously, endogenous mechanisms of cerebral protection and repair are activated in the physiological response to brain injury (Zhang et al., 2021; Askenase and Sansing, 2016). Clinical observation has also shown that some patients with an ICH show better recovery than others with similar characteristics, suggesting more effective repair mechanisms in these patients. Some of those mechanisms might be mediated by proteins with trophic/restorative or immunomodulatory action that are contained in circulating extracellular vesicles (EVs) (Hirsch et al., 2022).

EVs are endosomal-derived particles with a lipid membrane that are secreted by cells for intercellular signaling by transferring various molecular constituents, including micro-RNA and proteins (Abels and Breakefield, 2016). They can be detected in serum and in other body fluids and can cross the blood-brain barrier (Colombo et al., 2014), are involved in physiological and pathological conditions, and have been proposed to participate in mechanisms of brain repair in ischemic stroke (Otero-Ortega et al., 2021). Also, EVs might be involved in signaling between the immune system and the brain in response to ICH (Li et al., 2021a). In recent years, EVs have been studied as a potential therapeutic agent in preclinical models of ICH, showing promising results; however, those findings have yet to be translated to the clinical setting (Hirsch et al., 2022; Feng et al., 2022; Ding et al., 2021; Duan et al., 2020a; Zou et al., 2023; Laso-García et al., 2023a).

It could be postulated that the recovery process after ICH depends on a balance between brain damage and repair mechanisms or brain plasticity. Understanding the cellular events occurring in the recovering patient could help to pinpoint potential target mechanisms for interventional studies aimed at enhancing recovery after ICH. We hypothesize that, if EVs have a role in the repair process, there might be differences in the amount of circulating EVs and their protein cargo among patients, depending on their functional outcome.

Therefore, we performed a study aiming to describe the changes over time in the protein content of circulating EVs from patients with good and poor outcomes after ICH as an approach to unraveling the biological pathways underlying the repair processes of this disease.

2. Material and methods

We conducted a prospective observational study in patients with acute ICH admitted to the Stroke Unit or Intensive Care Unit of La Paz University Hospital between March 2018 and January 2021. We selected patients with spontaneous supratentorial ICH in the first 24 h from onset. Exclusion criteria were defined as traumatic or infratentorial ICH, signs of herniation or hydrocephalus on baseline computed tomography (CT) scan, or very severe or large ICH with short-term bad prognosis, previous history of stroke or ICH, previous functional deficits defined as a modified Rankin Scale (mRS) >1, severe comorbidities with short-term life expectancy, or participation in clinical trials with pharmacological intervention.

All patients were treated according to standard clinical protocols that follow current guidelines (Greenberg et al., 2022; Sandset et al., 2021) and underwent a similar rehabilitation regimen throughout the process. Participants or their proxies voluntarily agreed to participate by signing a written informed consent before inclusion. The study was approved by the Clinical Research Ethics Committee of La Paz University Hospital (PI-3093).

2.1. Variables and data collection

Demographic details and clinical variables were registered. Blood samples for EV isolation were collected at 24 h and 7 days (Fig. 1).

All patients underwent a non-enhanced CT scan on admission for diagnosis of ICH and a follow-up CT scan at 5–7 days to assess any change in hematoma volume. Additional imaging was obtained in case of clinical worsening at the discretion of the treating physician. ICH etiology, location, volume, and existence of intraventricular bleeding were registered.

After hospital discharge, patients completed visits at 3 and 6 months, during which medical complications, National Institutes of Health Stroke Scale (NIHSS) score, and functional deficits (as measured by mRS) were recorded.

At the end of the follow-up period, patients were divided into 2 groups depending on their functional outcome. Good recovery was defined as an improvement of more than 10 points or more than 50 % in the NIHSS score compared with baseline and an mRS of 0–2 at 6 months from onset.

2.2. Blood sampling, extracellular vesicle isolation and characterization

EVs were obtained from blood samples collected at 24 h and at 7 days after ICH onset. Nine mL of venous blood was collected in serum-separator tubes at both time points and centrifuged at 3000*g* at 4 °C for 15 min. Then, 4 mL of serum was aliquoted and stored at −80 °C until analysis. EVs were isolated from 250 μL of serum using an ExoQuick Ultra EV isolation kit (System Biosciences, USA) according to manufacturer's instructions. Isolated EVs were stored at −80 °C.

For EV characterization, 3 methods were used as recommended by the International Society for Extracellular Vesicles: western blot; nanoparticle tracking analysis (NTA); and transmission electron microscopy (TEM) (Théry et al., 2018). The methodology has been previously described (Laso-García et al., 2023a; Laso-García et al., 2023b) and is summarized below:

Western blot was performed using specific EV antibodies: anti-CD9 (1:750, Invitrogen, USA), anti-CD81 (1:250, Invitrogen, USA), anti-CD63 (1:1000, Invitrogen, USA), and anti-albumin antibody (1:1000, Invitrogen, USA) as a purity control. This was followed by a horseradish peroxidase secondary antibody (1:10000, Abcam). ECL Pierce chemiluminescence (Thermo Fisher Scientific, USA) was used for image acquisition.

EV size was studied through NTA with a NanoSight LN10 instrument (Malvern Instruments, UK). EVs were diluted in 500 μL of sterile

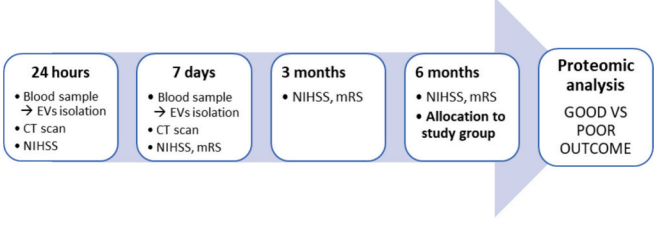

Fig. 1. Study workflow. EV: extracellular vesicles, NIHSS: National Institutes of Health Stroke Scale, mRS: modified Rankin Scale, CT: computed tomography.

phosphate-buffered saline (PBS) for a working concentration of 1 × 10^7–10^9 particles/mL, and 3 videos of 60 s were captured, with a shutter speed of 30 ms and a camera level of 13 (detection threshold of 3).

EV samples were analyzed by transmission electron microscopy with negative staining. The EV particles were applied to glow discharged collodion 300 mesh carbon-coated microscopy copper grids for 5 min, fixed for 5 min on a drop of PBS and 2 % paraformaldehyde, washed 2 times with MilliQ water, and negatively stained with 2 % aqueous uranyl acetate for 1 min. The samples were imaged on an FEI Tecnai 12 electron microscope equipped with an LaB6 filament operated at 120 kV. Images were recorded with an FEI Ceta digital camera at a nominal magnification of 30,000 × .

2.3. Extracellular vesicle quantification

For the EV quantification, we employed an ExoELISA-ULTRA assay kit (System Biosciences, USA). This kit, based on anti-CD63 antibodies, is specifically designed for the detection of tetraspanin CD63, a widely recognized EV marker (Laso-García et al., 2023a; Laso-García et al., 2023b; Rajeev Kumar et al., 2024; Gao et al., 2024).

2.4. Proteomics analysis of extracellular vesicle content

After the EVs were isolated, samples were mixed with a lysis buffer (4 % sodium dodecyl sulfate, 100 mM Tris pH 7.6, and 0.1 mM dithiothreitol) in a 1:1 ratio and incubated at 95 °C for 5 min (Abramowicz et al., 2018) to obtain their protein cargo. These proteins were then processed for protein identification and sequential window acquisition of all theoretical mass spectra (SWATH) library creation by liquid chromatography–tandem mass spectrometry (LC-MS/MS) using a data-dependent acquisition (DDA) method, and for protein quantification by LC-MS/MS using a data independent acquisition (DIA)-SWATH-MS method. For the DDA LC/MS-MS qualitative analysis, 4 μg of digested peptides were separated using reverse-phase chromatography. Data acquisition was performed with a TripleTOF 6600 System (SCIEX, Foster City, CA, USA), using a data-dependent workflow.

For relative quantification by SWATH-MS, we first built a spectral library. To construct the spectral libraries, peptide solution pools of each condition were analyzed with a shotgun DDA approach by micro-LC-MS/MS. These runs searched together against the human specific UniProt database (UniProt release 2020_01 Published on February 26, 2020; 20,365 human proteins) to obtain the SWATH library.

The false discovery rate (FDR) was set to <1 % for both peptides and proteins. Only peptides with a confidence score above 99 % were included in the spectral library.

Individual samples were then analyzed using the SWATH-MS acquisition method, which was created based on the ions present in the library. Once the samples were run individually using the SWATH-MS method, targeted data extraction of the fragment ion chromatogram traces from the SWATH-MS runs was performed with PeakView (version 2.2) using the SWATH Acquisition MicroApp (version 2.0). SWATH-MS quantitation was attempted for all proteins identified by ProteinPilot in the ion library with an FDR <1 %. PeakView computed an FDR and score for each assigned peptide according to the chromatographic and spectral components. Peptides with an FDR <5 % were used for protein quantitation, which was calculated by adding the peak areas of the corresponding peptides.

The integrated peak areas were exported to MarkerView software (AB SCIEX) for relative quantitative analysis. To control for possible uneven sample loss across the various samples during the preparation process, we performed a global normalization based on the total sum of all the peak areas extracted from all the peptides and transitions across the replicates of each sample. Multivariate statistical analysis using principal component analysis (PCA) was performed to compare data across samples.

Full details about the proteomic analysis methodology are available as Supplementary Material and in previous works published by our group (Laso-García et al., 2023a; Laso-García et al., 2023b).

2.5. Statistical analysis

Analyses and data representation were performed using R version 4.3.0 (*R: The R Project for Statistical Computing*, 2023). We performed descriptive statistics for baseline, imaging, and demographic data. For continuous variables, median and IQR or mean and SD values were obtained. For categorical variables, we calculated proportions by dividing the number of events by the total number of patients, excluding missing or unknown cases. Comparisons of quantitative variables between groups were made with Student's *t*-test or the Mann–Whitney *U* test, depending on data distribution. Associations between categorical variables were analyzed with Fisher's exact test or the χ^2 test as appropriate. For associations between continuous variables, Spearman's rank correlation coefficient was used.

The results from the proteomics studies were analyzed using SWATH principal component analysis (PCA) and cluster analysis, and "base", "stats", "ggplot2", "Hmisc", "dplyr" and "car" packages. The PCA was applied, considering the correlation matrix due to its pairwise two-sided *p*-values being 0 for the entire matrix. For the cluster analysis, Student's *t*-test for means comparison between samples was applied, employing Euclidean distance, suitable for quantitative variables and complete linkage as clustering criteria.

The EVs were sorted into 2 groups according to patient outcomes at 6 months, as previously established. Our analysis then focused on discerning changes in protein abundance between the 24-h and 7-day time points within each group. For the selection of differentially abundant proteins, we chose those with a fold change >2 or < 0.5 and a *p*-value <0.05. For functional analysis of the proteins with differential abundance, we used the Funrich analysis tool (Fonseka et al., 2021) and Reactome pathway analysis tool (Fabregat et al., *2018)*, along with functional annotations from the UniProt database (Bateman et al., 2023).

3. Results

3.1. Patient characteristics

A total of 48 patients with acute ICH were included in the study. One patient died in the first week, and 3 patients were lost to follow-up. The 44 (91.67 %) remaining patients completed the 6-month follow-up and were included in the final analysis (Fig. 2). Of these patients, 16 (36 %) had a good outcome according to the pre-defined criteria.

The patients' baseline characteristics are shown in Table 1. Patients with good outcomes were younger, had a smaller volume of hemorrhage on baseline CT scan, and had less severe neurological deficits, as measured by NIHSS score. The etiology was similar in both groups, with most patients having ICH related to hypertension. Of the 44 patients, 7 (15.9 %) had previously been on anticoagulation.

Thirty-nine percent (11/28) of the patients with poor outcomes had early neurological complications, such as intracranial hypertension or seizures, whereas none of the patients in the good outcome group did. Only 2 patients needed surgical intervention, which required external ventricular drainage, and 5 required intubation. All the patients with ICH related to anticoagulants had poor outcomes, even though anticoagulation was reverted in all cases. At the end of the study period, 7/44 (15.9 %) patients had died.

3.2. EV characterization

The isolated EVs showed typical morphology and size (<200 nm) by TEM and NTA, and they expressed specific proteins, as shown by western blot (Fig. 3).

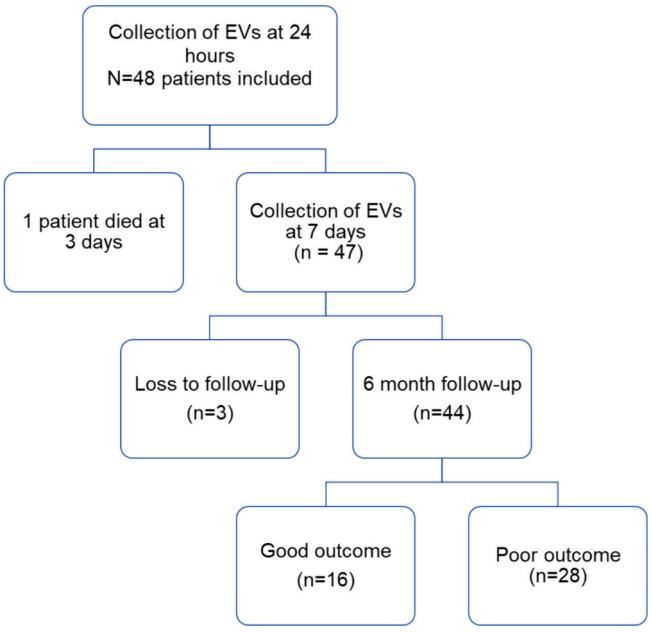

Fig. 2. Flowchart of patients included in the study.

Table 1
Clinical and demographic characteristics of the patients. LDL: low-density lipoprotein, ICH: intracerebral hemorrhage, NIHSS: National Institutes of Health Stroke Scale.

	Poor outcome	Good outcome	p
N	28	16	
Age mean (SD)	72.71 (11.11)	60.38 (13.69)	**0.002**
Female n (%)	9 (32.1)	6 (37.5)	0.976
Hypertension n (%)	23 (82.1)	12 (75.0)	0.860
Dyslipidemia n (%)	15 (53.6)	5 (31.2)	0.265
Diabetes mellitus n (%)	5 (17.9)	3 (18.8)	1.000
Atrial fibrillation n (%)	7 (25.0)	0 (0.0)	0.080
Diastolic blood pressure mean (SD)	91.41 (12.83)	102.06 (16.68)	**0.024**
Systolic blood pressure mean (SD)	173.63 (26.25)	183.62 (37.36)	0.309
Glycemia 24 h mean (SD)	111.84 (32.59)	102.40 (26.51)	0.349
Platelets 24 h mean (SD)	190,578.37 (76,655.09)	216,341.00 (115,098.87)	0.383
Creatinine 24 h mean (SD)	0.77 (0.31)	0.86 (0.56)	0.501
LDL 24 h mean (SD)	95.35 (28.46)	110.62 (25.13)	0.126
Lesion side = left n (%)	17 (60.7)	12 (75.0)	0.528
Intraventricular n (%)	14 (50.0)	2 (12.5)	**0.031**
ICH volume at baseline mean (SD)	19.48 (15.55)	5.62 (3.05)	**0.001**
ICH volume at 7 days mean (SD)	20.86 (15.74)	4.58 (1.77)	**<0.001**
Baseline NIHSS median (IQR)	19 (11.75, 22.00)	8.0 (6.75, 12.25)	**<0.001**
Infection in first week n (%)	13 (46)	3 (18.7)	0.104
Etiology n (%)			0.585
Amyloid angiopathy	3 (10.7)	2 (12.5)	
Hypertension	22 (78.5)	11 (68.8)	
Idiopathic	3 (10.7)	2 (12.5)	
Vascular malformation	0 (0.0)	1 (6.2)	

3.3. Number of extracellular vesicles

No significant differences were found between the concentration of EVs at 24 h ($1.67 \times 10^6 \pm 1.93 \times 10^6$ EVs/mL) and 7 days ($1.44 \times 10^6 \pm 1.84 \times 10^5$ EVs/mL, $p > 0.05$) in the entire patient cohort. Patients with good outcomes had higher levels of EVs at 24 h compared with patients with poor outcomes (2.09×10^6 vs 1.43×10^6, $p = 0.03$), but this difference was lost at 7 days (Fig. 4A).

We found no significant relationship between EV levels and patients' sex, age, ICH volume, or NIHSS score on admission (Fig. 4).

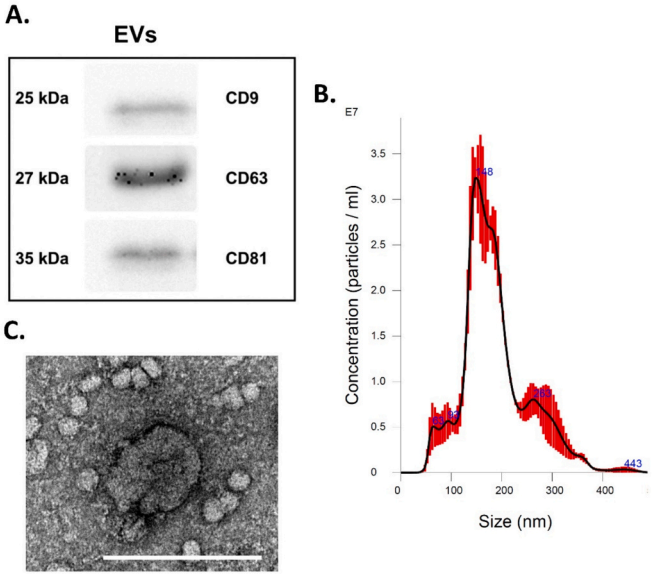

Fig. 3. Extracellular vesicle (EV) characterization by (A) western blot showing presence of specific EV proteins (CD9, CD81, CD63); (B) nanoparticle tracking analysis; and (C) transmission electron microscopy imaging. Scale bar: 200 nm. EVs, extracellular vesicles; kDa, kilodalton.

3.4. Extracellular vesicle protein content

In the proteomic analysis of EV cargo from the entire patient cohort, a total of 1321 proteins were identified. In the functional enrichment and pathway analysis of all the identified proteins, we found that the biological processes with the greatest representation were complement function, hemostasis, and immune response (both innate and adaptative). There were also proteins related to peptide metabolism, transport, RNA processing and translation, and cell-to-cell signaling. Also, several proteins were associated with axon guidance and nervous system development (Fig. 5) (Table 2).

3.5. Differential abundance analysis of protein content

We then performed an analysis of the differential protein abundance along the predefined study time-points in each of the patient groups (Fig. 6). Full results from the differential abundance analysis are available in Supplemental Material 2. In Supplemental Material 3, we include a description of the proteins with differential abundance and the main functions associated with them.

In the patients with poor outcomes, there were 12 proteins with differential abundance (Fig. 7). Among them, those that were more abundant at 7 days compared with 24 h included acute-phase reactants and proteins associated with inflammation, such as C-reactive protein (CRP) (FC = 2.19, $p = 0.036$) and serum amyloid A-2 protein (SAA2) (fold change [FC] = 2.1, p = 0.03). There was also galectin-7 (LEG-7), a protein associated with pro-apoptotic processes (FC = 3.5, $p = 0.019$), and SEC13 protein, which is involved in the MTOR pathway (FC = 2.87, $p < 0.001$).

In patients with good outcomes, we found 25 proteins with differential abundance in EVs at 7 days compared with 24 h (Fig. 7). There were 15 down-regulated proteins, which included immunoglobulins and proteins related to innate immunity and cell migration, such as peptidoglycan recognition protein 1 (PGRP1) (FC = 0.4, $p = 0.014$), neutrophil defensin 1 (DEF1) (FC = 0.34, $p = 0.001$), and bridging

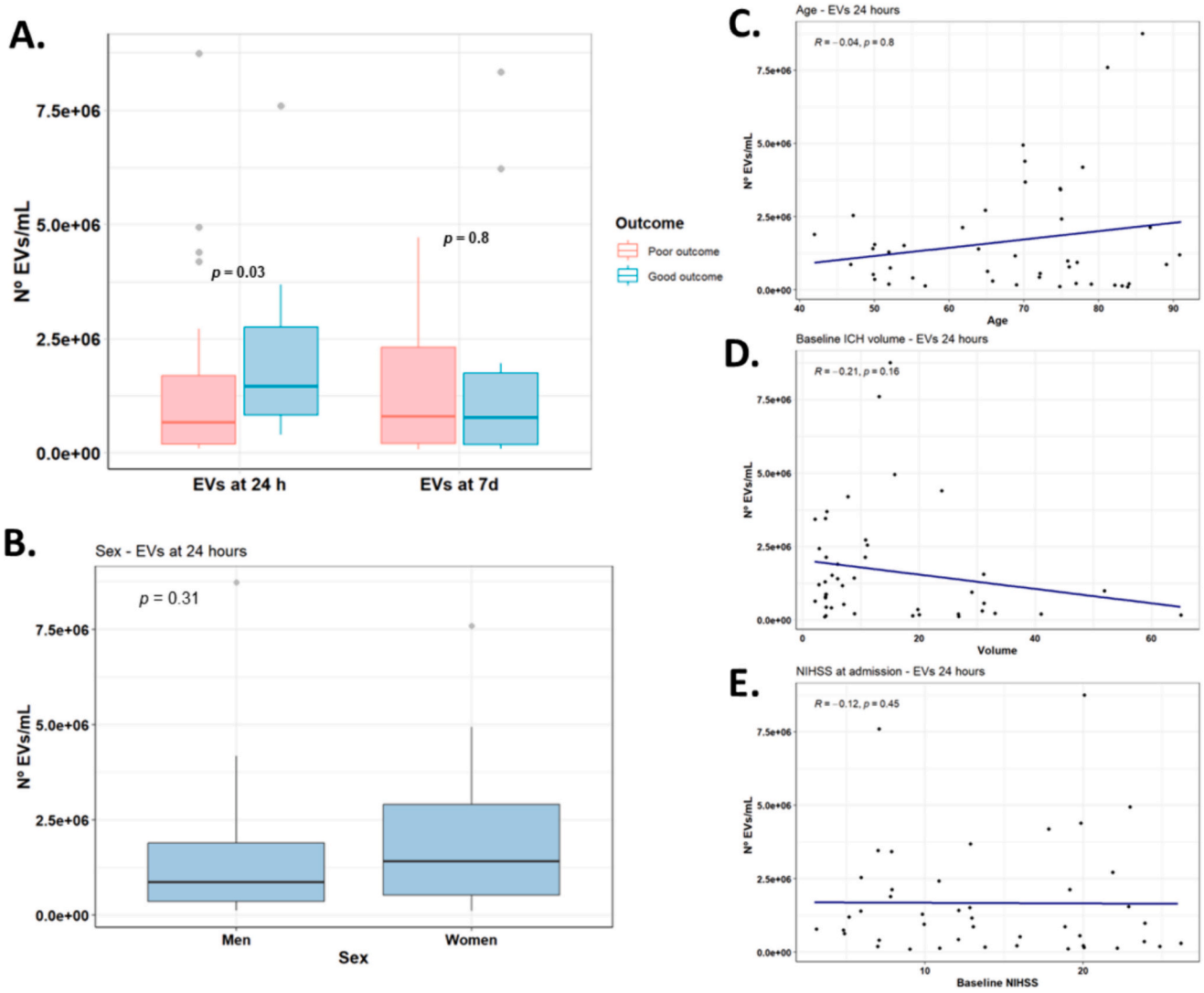

Fig. 4. (A) Boxplot showing number of EVs in both groups at each time point. (B) Boxplot showing number of EVs in relation to sex. (C) EV levels in relation to age. (D) EV levels in relation to ICH volume at admission. (E) EV levels in relation to NIHSS score at admission. EVs: extracellular vesicles; R: Spearman's rank correlation coefficient.

integrator 2 (BIN2) (FC = 0.448, p = 0.01).

There were also 10 proteins with increased abundance at 7 days, some associated with immunomodulation, apoptosis regulation, stress response, neurogenesis, and angiogenesis. Attractin (ATRN) (FC = 2.02, $p = 0.03$) and pantetheine hydrolase VNN2 (VNN2) regulate inflammatory response (FC = 2.18, $p = 0.046$); mitochondrial import receptor subunit TOM34 (TOMM34) participates in metabolism and in the reduction of oxidative stress (FC = 2.099, $p = 0.004$); deoxyribose-phosphate aldolase (DERA) (FC = 2.29, 0.015) and xanthine dehydrogenase/oxidase are also involved in oxidative stress response (FC = 2.25, $p = 0.029$); Guanine nucleotide-binding protein G(i) subunit alpha-2 (GNAI2) is involved in thrombosis and apoptosis modulation (FC = 2.04, $p = 0.015$); and Rho gap activating protein (RHG01) is involved in numerous metabolic processes including angiogenesis and neurogenesis (FC = 2.06, $p = 0.005$).

4. Discussion

To the best of our knowledge, this study represents the first comprehensive exploration of the protein cargo of EVs in individuals with ICH. The study of circulating EVs provides a means of peripherally assessing the biological processes that are triggered as a response to a given condition, and this particular work provides relevant information to increase knowledge of ICH pathophysiology.

EVs were collected at 24 h and 7 days to capture the evolving dynamics from 2 different stages of the disease. The findings at earlier stages could reflect primary tissue damage processes, whereas at later stages they might manifest mechanisms involved in waste removal and tissue protection and repair, aligning with clinical evolution. Analyzing the changes between these 2 time points could improve our understanding of these mechanisms.

We found no association between EV levels and well-established prognostic factors, such as ICH volume, age, or NIHSS score, factors that in our series were higher in patients with poor outcomes. This, together with the finding that patients with good outcomes tend to have higher levels of circulating EVs at earlier stages after ICH, suggests that the number of EVs does not depend on disease severity, and supports the hypothesis that EVs might be involved in processes triggered as a response to the damage that can be related to brain protection and repair. A prior study had reported that the quantity of EVs in patients with ICH, when combined with other clinical parameters, can predict overall patient outcomes, a finding consistent with our results (Sawant et al., 2022). In the subacute phase, no differences were found in the number of circulating EVs in relation to outcomes.

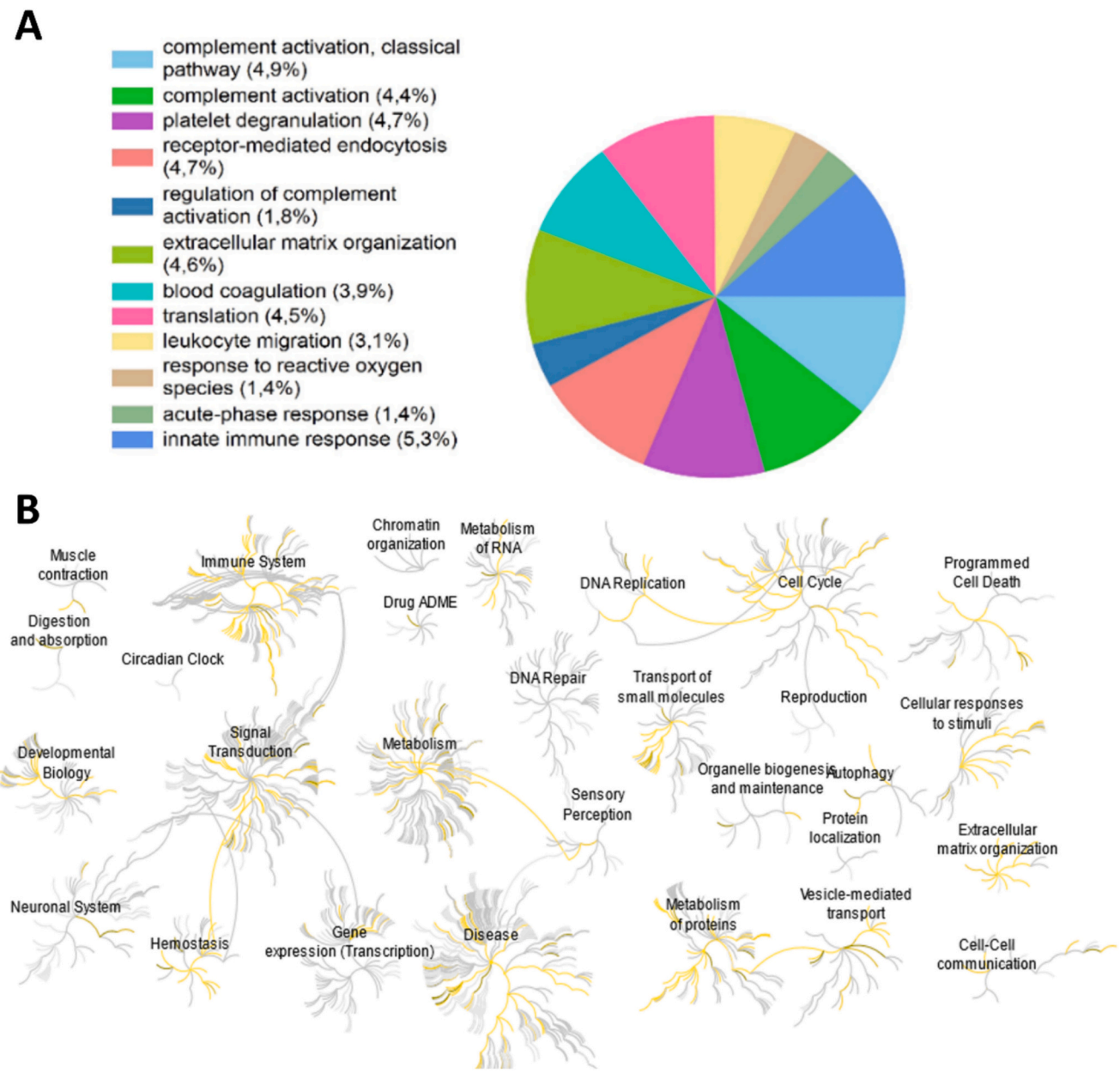

Fig. 5. Representation of the most relevant biological processes associated with the proteins identified in EVs from the global patient cohort according to the (A) Funrich analysis and (B) Reactome pathway analysis tool, with yellow lines highlighting the pathways that were overrepresented among the identified proteins. (For interpretation of the references to colour in this figure legend, the reader is referred to the web version of this article.)

The key findings from our study concern the protein content of EVs. In both patients with good and poor outcomes we found changes in the protein content between the predefined study time points; however, the nature of these changes in the proteomic profile differed significantly between the 2 groups.

In the patients with poor outcomes, there was an increased abundance of proteins associated with inflammation at 7 days compared with 24 h. Proteins such as CRP and SAA2 are well known acute-phase reactants and have been previously associated with poor outcomes in patients with ICH (Di Napoli et al., 2011; Pathak and Agrawal, 2019; Sack, 2018; Huangfu et al., 2020). This finding suggests that patients with poor outcomes experience an enhanced and persistent inflammatory response that could potentially contribute to secondary brain injury and cellular damage, hindering their recovery. The presence of LEG-7, an intracellular protein that has a pro-apoptotic function (Kuwabara et al., 2002), could also point to more cellular damage.

On the other hand, in the good outcomes group, proteins like PGRP1 and DEF1, which are related to the innate immune response, show a decrease at 7 days that does not occur in patients with poor outcomes. In the first stages of ICH the damage caused by the hematoma triggers a local immune response, with activation of microglia and recruitment of inflammatory leukocytes (Askenase and Sansing, 2016). This initial inflammation is one of the mechanisms that later leads to the secondary injury cascade in ICH pathophysiology (Zhang et al., 2022). The findings in patients with good outcomes suggest a reduction in the innate immune response from the early phase of ICH to the later stage that might result in less tissue damage, whereas patients with poor outcomes could fare worse due to a prolonged inflammatory state secondary to persistent activation of the innate immune response. We also cannot rule out that these proteins in the EVs might be linked to the initial severity of the hemorrhage; thus, patients with more severe ICH would have greater and longer-lasting innate immunity activation, whereas the decrease in

Table 2
The most relevant pathways with overrepresentation identified from Reactome enrichment analysis, sorted by *p*-value.

Pathway name	Entities					Reactions		
	Found	Total	Ratio	*P* value	FDR	Found	Total	Ratio
Eukaryotic translation elongation	53	95	0.008	1.11E-16	7.33E-15	*9*	*9*	*0.001*
Peptide chain elongation	50	90	0.008	1.11E-16	7.33E-15	*5*	*5*	*0*
Eukaryotic translation termination	50	94	0.008	1.11E-16	7.33E-15	*5*	*5*	*0*
Nonsense mediated decay (NMD) independent of the exon junction complex (EJC)	51	96	0.008	1.11E-16	7.33E-15	*1*	*1*	*0*
Formation of a pool of free 40S subunits	54	102	0.009	1.11E-16	7.33E-15	*2*	*2*	*0*
Complement cascade	75	146	0.012	1.11E-16	7.33E-15	*72*	*72*	*0.005*
Regulation of complement cascade	69	135	0.011	1.11E-16	7.33E-15	*42*	*42*	*0.003*
GTP hydrolysis and joining of the 60S ribosomal subunit	57	113	0.01	1.11E-16	7.33E-15	*3*	*3*	*0*
Cap-dependent translation initiation	58	120	0.01	1.11E-16	7.33E-15	*18*	*18*	*0.001*
Nonsense-mediated decay (NMD)	54	117	0.01	1.11E-16	7.33E-15	*6*	*6*	*0*
Nonsense mediated decay (NMD) enhanced by the exon junction complex (EJC)	54	117	0.01	1.11E-16	7.33E-15	*5*	*5*	*0*
Neutrophil degranulation	189	478	0.041	1.11E-16	7.33E-15	*10*	*10*	*0.001*
Eukaryotic translation initiation	58	120	0.01	1.11E-16	7.33E-15	*20*	*21*	*0.001*
Platelet degranulation	73	128	0.011	1.11E-16	7.33E-15	*10*	*11*	*0.001*
Binding and uptake of ligands by scavenger receptors	59	129	0.011	1.11E-16	7.33E-15	*30*	*33*	*0.002*
Response to elevated platelet cytosolic Ca2+	73	133	0.011	1.11E-16	7.33E-15	*10*	*14*	*0.001*
Platelet activation, signaling and aggregation	92	265	0.023	1.11E-16	7.33E-15	*80*	*119*	*0.008*
L13a-mediated translational silencing of ceruloplasmin expression	57	112	0.01	1.11E-16	7.33E-15	*2*	*3*	*0*
Hemostasis	189	727	0.062	1.11E-16	7.33E-15	*224*	*342*	*0.024*
Innate immune system	314	1198	0.102	1.11E-16	7.33E-15	*362*	*703*	*0.048*

patients with a good outcome could indicate lesser initial severity.

There were also several proteins with higher abundance at 7 days in the good outcome group. These proteins are described as being involved in a wide variety of biological processes; however, given that we did not find any previous studies describing them in the ICH setting, further investigation is needed to determine their specific roles. Nevertheless, given the functions of some of the proteins in this group, we consider it plausible that they could play a role in recovery.

ATRN is a molecule secreted by activated T cells, involved in initial immune cell clustering during the inflammatory response, and promoting T cell activation by interaction with macrophages (Duke-Cohan et al., 1998; Duke-Cohan et al., 2000). Although the potential role of ATRN in this specific context is uncertain, its presence in the good outcome group could point to an involvement in the mechanisms that control inflammation. ATRN is also involved in central nervous system myelination, and its absence in the brain has been associated with neurodegeneration (Li et al., 2021b; Tang and Duke-Cohan, 2002; Shahrour et al., 2017); thus, it could also have a protective role and participate in repair processes.

RHG01 could also be of relevance. Rho GTPase-activating proteins are a ubiquitous family of multifunctional molecules that transduce diverse intracellular signals by regulating Rho GTPase activities in various pathways. They are involved in angiogenesis, neurogenesis, and synapsis development processes (Moon and Zheng, 2003). They are important in the context of vascular biology because they influence endothelial barrier function, vascular smooth muscle contractility and proliferation, and vascular function and remodeling (Eckenstaler et al., 2022; Eisa-Beygi et al., 2021). Given that they have been reported to participate in coagulation and platelet activation processes *(Elvers, 2016; Comer, 2022),* their increased abundance in patients with ICH could be related to an activation of endothelial repair and hemostasis mechanisms, contributing to the repair of vascular damage.

Another protein considered relevant is GNAI2. It belongs to the G(i) protein group and serves as a modulator or transducer in various transmembrane signaling systems. It has a potential role in cell division and has been associated with cell proliferation and apoptosis inhibition (Cho and Kehrl, 2007; Arang and Gutkind, 2020). It also appears to be involved in platelet activation and has been associated with thrombotic damage in animal models of ischemia (Devanathan et al., 2015; von Kügelgen, 2017). In the ICH setting, this prothrombotic effect could be beneficial for hemostasis.

Some other proteins with increased abundance in patients with good outcomes are involved in the reduction of oxidative damage. After ICH there is an increase of reactive oxygen species, and oxidative stress is one of the main mechanisms leading to secondary brain injury; thus, the presence of these proteins could contribute to a reduction of this type of damage. DERA converts 2-deoxy-D-ribose-5-phosphate into glyceraldehyde-3-phosphate and acetaldehyde. A study had shown that it allows ATP production in conditions of energy deprivation, activating a pathway that could allow some cells to minimize or delay stress-induced damage (Salleron et al., 2014). VNN2, which belongs to the Vanin family of proteins involved in the metabolism of vitamin B5, have also been reported to have a possible role in promoting tissue repair under conditions of oxidative stress (Martin et al., 2001). Vanin proteins have also been associated with the regulation of cell adhesion, migration, and neutrophil motility (Martin et al., 2001); therefore, it could have a role as a modulator of neutrophil activity and inflammatory response in ICH.

TOMM34 plays a relevant role in mitochondria protein import and is involved in multiple metabolic pathways, including DNA replication and repair and oxidative phosphorylation (Poverennaya et al., 2023). Given that it has also been linked to activated T CD4+ cells, modulating mitochondrial activity, and the management of reactive oxygen species in these cells (Gerner et al., 2019), it could also be associated with the response to oxidative stress or with the immune response in patients with ICH.

Preclinical research has shown that the protein content of circulating EVs reflects evolutionary changes in the pathophysiology of ICH, with a greater abundance of proteins related to cellular damage response in early stages, whereas proteins involved in the healing and repair processes are upregulated in the subacute phase (Laso-García et al., 2023b). Also, a differential abundance of proteins in EVs depending on outcomes has been demonstrated in a preclinical model of ICH, with EVs from animals with good recovery having lower levels of proteins involved in immune system activation pathways and inflammation, among others related to better tissue preservation (Laso-García et al., 2023a).

It has also been suggested that EVs might play a role in the processes of brain repair by transferring molecules involved in trophic and immunomodulatory functions, and previous studies have shown that EVs appear to promote plasticity in experimental models of stroke and modulate inflammation after ICH (Duan et al., 2020b). Particularly, our group has shown that intravenous administration of blood-derived EVs from both rats and humans who experienced spontaneous good recovery after ICH improves functional outcomes, white matter integrity, and histological markers of tissue repair in a preclinical proof-of-concept study (Laso-García et al., 2023a).

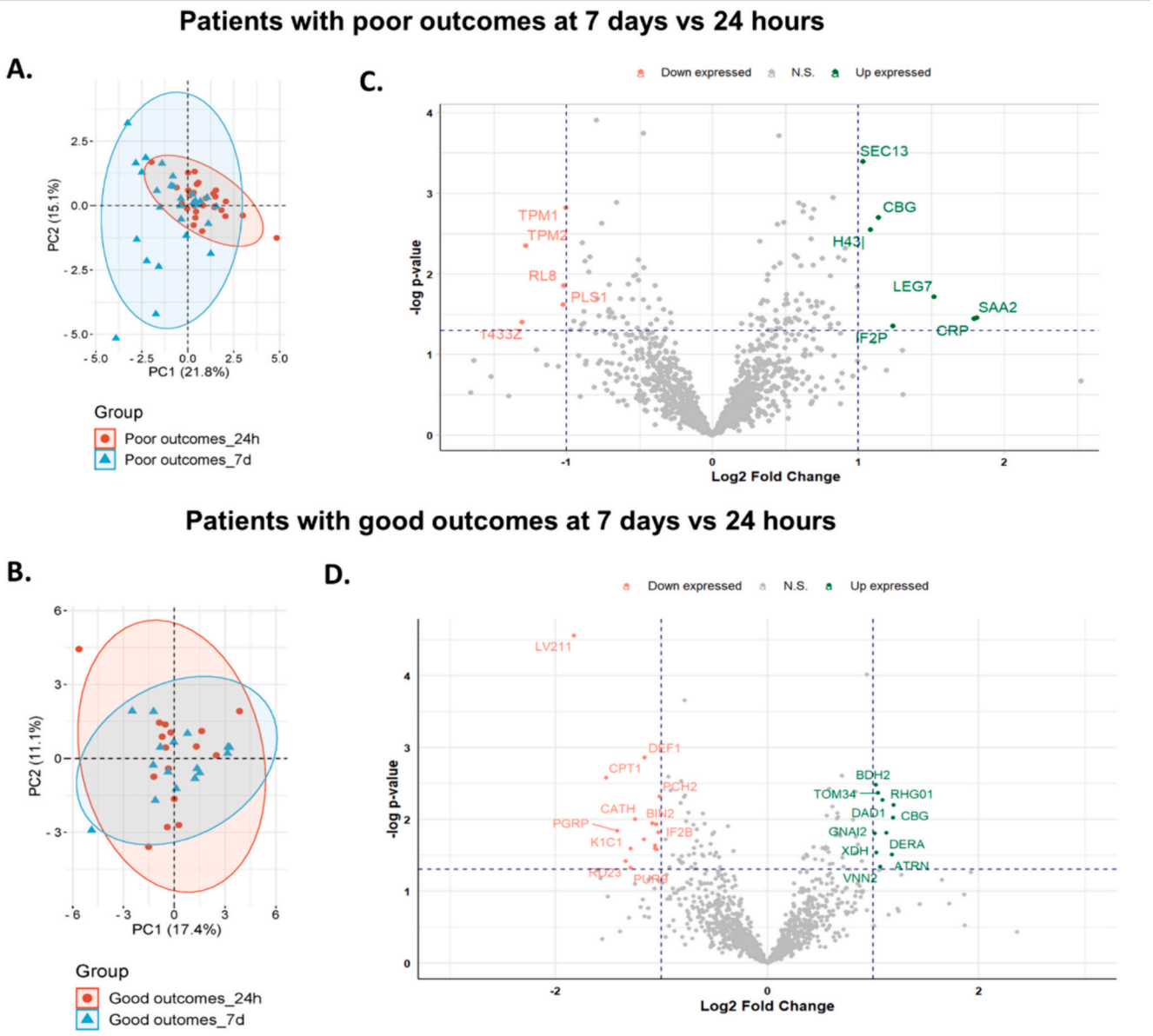

Fig. 6. (A, B) Principal component analysis for poor and good outcome groups at 7 days and 24 h. Principal component 1 (PC1) and principal component 2 (PC2) were identified by variance in the SWATH-MS Peakview data. The percentage indicates how much variance was explained by PC1 and PC2. (C, D) Volcano plots showing the proteins present in EVs by time point comparisons in each patient group. The cut-offs for significant changes are FC >2 or < 0.5 and $P < 0.05$. Red spots show proteins with decreased abundance at 7 days, green spots show proteins with increased abundance at 7 days, and gray spots show proteins with no differential abundance between both time points. (For interpretation of the references to colour in this figure legend, the reader is referred to the web version of this article.)

The results from the present study align with the preclinical data and support the hypothesis that circulating EVs and their protein content could be biomarkers of the pathophysiological processes underlying ICH. This opens a promising venue for the development of new therapies aimed at improving recovery after ICH.

Several limitations should be acknowledged. First, the sample size of the 2 groups limits the power of the study. There is an inherent variability in the clinical characteristics and the degree of disease severity, which could have influenced the EV protein content. To reduce this potential bias associated with individual variability, we chose to focus our analysis on the changes in protein cargo over time in each of the patient groups, rather than directly comparing patients with different outcomes.

Also, mass spectrometry is widely used for protein identification and quantification in proteomics; however, the complexity of proteomic instrumentation introduces potential sources of variability. One limitation of DDA is the difficulty in identifying low-abundance peptides or peptides that are not selected for fragmentation, which can result in a loss of information. Consequently, there are likely more proteins involved that might not have been detected.

5. Conclusions

This study shows that the protein content of circulating EVs in patients with ICH changes over time and that this change differs depending on clinical outcome, with patients with good recovery showing a greater abundance of proteins possibly related to protection and repair processes such as modulation of inflammatory response or protection against oxidative stress, among others, and a lower abundance of inflammatory proteins in the sub-acute phase. Nevertheless, further research on the proteins described is needed to determine the biological pathways and molecular processes in which they are involved, to better

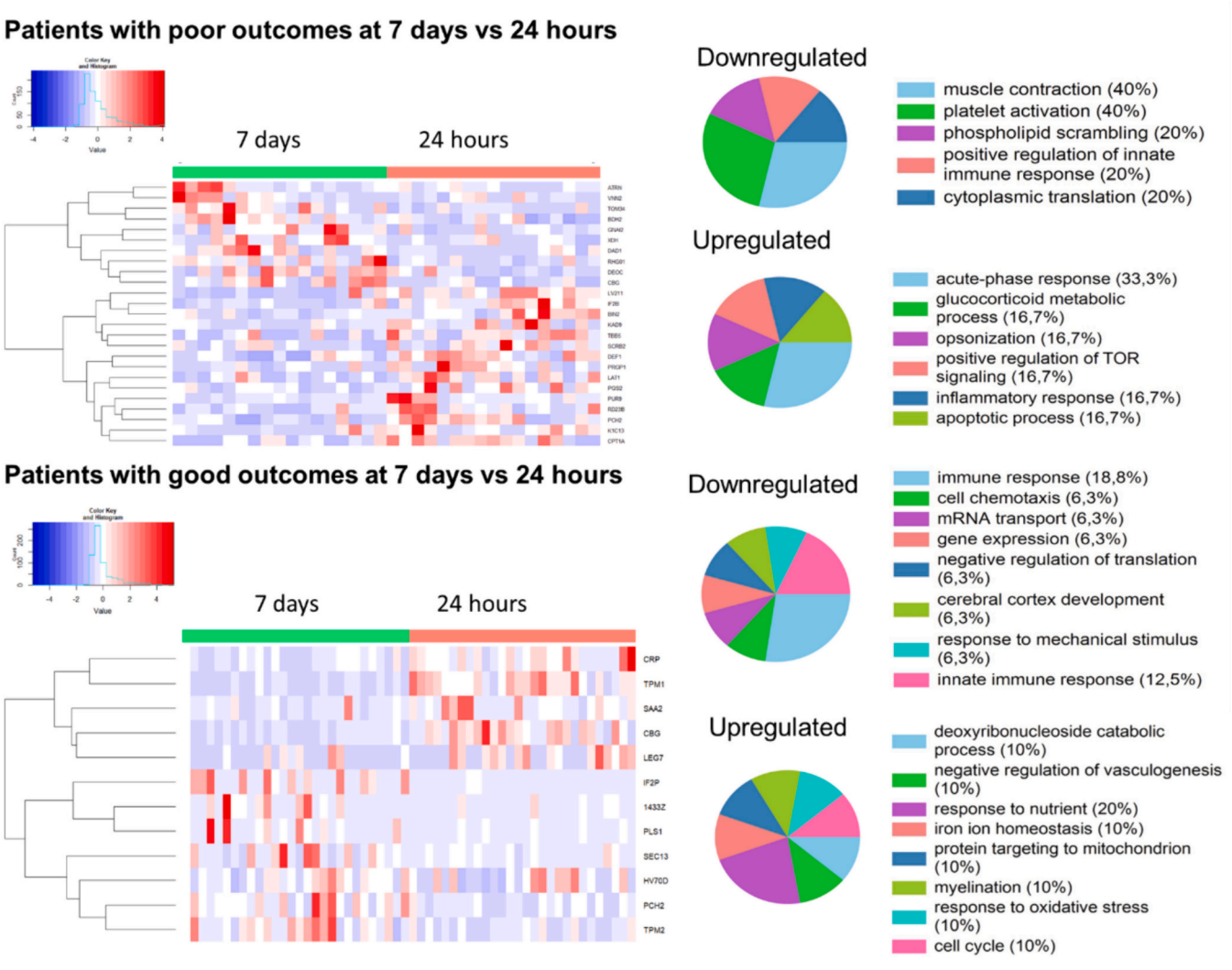

Fig. 7. Clustered heatmaps of normalized protein levels from the proteins with differential abundance by time comparisons in each outcome group. On the right, a representation of the most relevant biological processes in which the differential proteins are involved, according to Funrich analysis.

define their potential role in recovery and reach a clinical translation of these findings into therapies.

CRediT authorship contribution statement

Laura Casado-Fernández: Visualization, Methodology, Investigation, Formal analysis, Data curation, Writing – original draft. **Fernando Laso-García:** Visualization, Methodology, Investigation, Formal analysis, Data curation, Writing – original draft. **Dolores Piniella:** Methodology, Investigation, Formal analysis, Writing – review & editing. **Mari Carmen Gómez-de Frutos:** Supervision, Methodology, Investigation, Writing – review & editing. **Laura Otero-Ortega:** Supervision, Methodology, Investigation, Writing – review & editing. **Susana-Belén Bravo:** Methodology, Investigation, Formal analysis, Writing – review & editing. **Blanca Fuentes-Gimeno:** Methodology, Investigation, Writing – review & editing. **Félix Docando:** Methodology, Investigation, Formal analysis, Writing – review & editing. **Elisa Alonso-López:** Methodology, Investigation, Writing – review & editing. **Gerardo Ruiz-Ares:** Methodology, Investigation, Writing – review & editing. **Jorge Rodríguez-Pardo:** Methodology, Investigation, Writing – review & editing. **Ricardo Rigual:** Methodology, Investigation, Writing – review & editing. **Elena de Celis-Ruiz:** Methodology, Investigation, Writing – review & editing. **Carlos Hervás:** Methodology, Investigation, Writing – review & editing. **Exuperio Díez-Tejedor:** Supervision, Investigation, Writing – review & editing. **María Gutiérrez-Fernández:** Supervision, Resources, Project administration, Methodology, Investigation, Funding acquisition, Conceptualization, Writing – review & editing. **María Alonso de Leciñana:** Supervision, Resources, Project administration, Methodology, Investigation, Funding acquisition, Conceptualization, Writing – review & editing.

Declaration of competing interest

The authors have no conflicts of interest to disclose.

Data availability

The mass spectrometry proteomics data have been deposited to the ProteomeXchange Consortium via the PRIDE partner repository with the dataset identifier PXD048138.

Acknowledgments

This work was supported by Carlos III Health Institute (ISCIII) and co-funded by the European Union (European Regional Development Fund-FEDER) under grant PI17/01922 and PI20/00243, Invictus plus

network under grant RD16/0019/0005, RICORS ICTUS network under grant RD21/0006/0012 and the Next Generation EU fundig for actions in the Recovery and Resilience Mechanism, Miguel Servet under grant CPII20/00002 to MG-F; CP20/00024 to LO-O, Ministerio de Universidades, Plan de Recuperación, Transformación y Resiliencia y la Universidad Autónoma de Madrid under grant CA1/RSUE/2021-00753 to DP, and the Spanish Ministry of Health- (ISCIII) under grant CM20/00047 to EA-L, CM23/00022 to LC-F, FI18/00026 to FL-G and FI17/00188 to MG-dF.

We also thank the editing assistance of Morote Traducciones.

Appendix A. Supplementary data

Supplementary data to this article can be found online at https://doi.org/10.1016/j.nbd.2024.106665.

References

Abels, E.R., Breakefield, X.O., 2016. Introduction to extracellular vesicles: biogenesis, RNA cargo selection, content, release, and uptake. Cell. Mol. Neurobiol. 36 (3), 301. https://doi.org/10.1007/S10571-016-0366-Z.

Abramowicz, A., Marczak, L., Wojakowska, A., et al., 2018. Harmonization of exosome isolation from culture supernatants for optimized proteomics analysis. PLoS One 13 (10). https://doi.org/10.1371/JOURNAL.PONE.0205496.

Arang, N., Gutkind, J.S., 2020. G proteins and G protein coupled receptors as Cancer drivers. FEBS Lett. 594 (24), 4201. https://doi.org/10.1002/1873-3468.14017.

Askenase, M.H., Sansing, L.H., 2016. Stages of the inflammatory response in pathology and tissue repair after intracerebral hemorrhage. Semin. Neurol. 36 (3), 288. https://doi.org/10.1055/S-0036-1582132.

Bateman, A., Martin, M.J., Orchard, S., et al., 2023. UniProt: the universal protein knowledgebase in 2023. Nucleic Acids Res. 51 (D1), D523–D531. https://doi.org/10.1093/NAR/GKAC1052.

Cho, H., Kehrl, J.H., 2007. Localization of Gi alpha proteins in the centrosomes and at the midbody: implication for their role in cell division. J. Cell Biol. 178 (2), 245–255. https://doi.org/10.1083/JCB.200604114.

Colombo, M., Raposo, G., Théry, C., 2014. Biogenesis, secretion, and intercellular interactions of exosomes and other extracellular vesicles. Annu. Rev. Cell Dev. Biol. 30, 255–289. https://doi.org/10.1146/ANNUREV-CELLBIO-101512-122326.

Comer, S.P., 2022. Turning platelets off and on: role of RhoGAPs and RhoGEFs in platelet activity. Front. Cardiovasc. Med. 8. https://doi.org/10.3389/FCVM.2021.820945.

Devanathan, V., Hagedorn, I., Köhler, D., et al., 2015. Platelet Gi protein Gαi2 is an essential mediator of thrombo-inflammatory organ damage in mice. Proc. Natl. Acad. Sci. USA 112 (20), 6491–6496. https://doi.org/10.1073/PNAS.1505887112/-/DCSUPPLEMENTAL.

Di Napoli, M., Godoy, D.A., Campi, V., et al., 2011. C-reactive protein level measurement improves mortality prediction when added to the spontaneous intracerebral hemorrhage score. Stroke 42 (5), 1230–1236. https://doi.org/10.1161/STROKEAHA.110.604983.

Ding, H., Jia, Y., Lv, H., Chang, W., Liu, F., Wang, D., 2021. Extracellular vesicles derived from bone marrow mesenchymal stem cells alleviate neuroinflammation after diabetic intracerebral hemorrhage via the miR-183-5p/PDCD4/NLRP3 pathway. J. Endocrinol. Investig. 44 (12), 2685–2698. https://doi.org/10.1007/S40618-021-01583-8.

Duan, S., Wang, F., Cao, J., Wang, C., 2020a. Exosomes derived from MicroRNA-146a-5p-enriched bone marrow mesenchymal stem cells alleviate intracerebral hemorrhage by inhibiting neuronal apoptosis and microglial M1 polarization. Drug Des. Devel. Ther. 14, 3143–3158. https://doi.org/10.2147/DDDT.S255828.

Duan, S., Wang, F., Cao, J., Wang, C., 2020b. Exosomes derived from MicroRNA-146a-5p-enriched bone marrow mesenchymal stem cells alleviate intracerebral hemorrhage by inhibiting neuronal apoptosis and microglial M1 polarization. Drug Des. Devel. Ther. 14, 3143–3158. https://doi.org/10.2147/DDDT.S255828.

Duke-Cohan, J.S., Gu, J., Mclaughlin, D.F., Xu, Y., Freeman, G.J., Schlossman, S.F., 1998. Attractin (DPPT-L), a member of the CUB family of cell adhesion and guidance proteins, is secreted by activated human T lymphocytes and modulates immune cell interactions. Proc. Natl. Acad. Sci. USA 95 (19), 11336. https://doi.org/10.1073/PNAS.95.19.11336.

Duke-Cohan, J.S., Tang, W., Schlossman, S.F., 2000. Attractin: a cub-family protease involved in T cell-monocyte/macrophage interactions. Adv. Exp. Med. Biol. 477, 173–185. https://doi.org/10.1007/0-306-46826-3_20.

Eckenstaler, R., Hauke, M., Benndorf, R.A., 2022. A current overview of RhoA, RhoB, and RhoC functions in vascular biology and pathology. Biochem. Pharmacol. 206. https://doi.org/10.1016/J.BCP.2022.115321.

Eisa-Beygi, S., Vo, N., (Jack), Link BA., 2021. RhoA activation-mediated vascular permeability in capillary malformation-arteriovenous malformation syndrome: a hypothesis. Drug Discov. Today 26 (8), 1790–1793. https://doi.org/10.1016/J.DRUDIS.2020.12.012.

Elvers, M., 2016. RhoGAPs and rho GTPases in platelets. Hamostaseologie 36 (3), 168–177. https://doi.org/10.5482/HAMO-14-09-0046.

Fabregat, A., Sidiropoulos, K., Viteri, G., et al., 2018. Reactome diagram viewer: data structures and strategies to boost performance. Bioinformatics 34 (7), 1208–1214. https://doi.org/10.1093/BIOINFORMATICS/BTX752.

Feng, Zhou J., Xiong, Y., Kang, X., et al., 2022. Application of stem cells and exosomes in the treatment of intracerebral hemorrhage: an update. Stem Cell Res Ther 13 (1). https://doi.org/10.1186/S13287-022-02965-2.

Fonseka, P., Pathan, M., Chitti, S.V., Kang, T., Mathivanan, S., 2021. FunRich enables enrichment analysis of OMICs datasets. J. Mol. Biol. 433 (11) https://doi.org/10.1016/J.JMB.2020.166747.

Gao, H., Zeng, Y., Huang, X., et al., 2024. Extracellular vesicles from organoid-derived human retinal progenitor cells prevent lipid overload-induced retinal pigment epithelium injury by regulating fatty acid metabolism. J. Extracell Vesicles 13 (1). https://doi.org/10.1002/JEV2.12401.

Gerner, M.C., Niederstaetter, L., Ziegler, L., et al., 2019. Proteome analysis reveals distinct mitochondrial functions linked to interferon response patterns in activated CD4+ and CD8+ T cells. Front. Pharmacol. 10. https://doi.org/10.3389/FPHAR.2019.00727/FULL.

Greenberg, S.M., Ziai, W.C., Cordonnier, C., et al., 2022. 2022 guideline for the Management of Patients with Spontaneous Intracerebral Hemorrhage: a guideline from the American Heart Association/American Stroke Association. Stroke 53 (7), E282–E361. https://doi.org/10.1161/STR.0000000000000407.

Hirsch, Y., Geraghty, J.R., Reiter, C.R., et al., 2022. Unpacking the role of extracellular vesicles in ischemic and hemorrhagic stroke: pathophysiology and therapeutic implications. Transl. Stroke Res. https://doi.org/10.1007/S12975-022-01027-2. Published online.

Huangfu, X.Q., Wang, L.G., Di, Le Z., Tao, B., 2020. Utility of serum amyloid a as a potential prognostic biomarker of acute primary basal ganglia hemorrhage. Clin. Chim. Acta 505, 43–48. https://doi.org/10.1016/J.CCA.2020.02.022.

Kuwabara, I., Kuwabara, Y., Yang, R.Y., et al., 2002. Galectin-7 (PIG1) exhibits pro-apoptotic function through JNK activation and mitochondrial cytochrome c release. J. Biol. Chem. 277 (5), 3487–3497. https://doi.org/10.1074/JBC.M109360200.

Laso-García, F., Casado-Fernández, L., Piniella, D., et al., 2023a. Circulating extracellular vesicles promote recovery in a preclinical model of intracerebral hemorrhage. Mol. Ther. Nucleic Acids 32, 247–262. https://doi.org/10.1016/j.omtn.2023.03.006.

Laso-García, F., Piniella, D., Gómez-de Frutos, M.C., et al., 2023b. Protein content of blood-derived extracellular vesicles: an approach to the pathophysiology of cerebral hemorrhage. Front. Cell. Neurosci. 16 https://doi.org/10.3389/FNCEL.2022.1058546.

Li, M., Li, X., Wang, D., et al., 2021a. Inhibition of exosome release augments neuroinflammation following intracerebral hemorrhage. FASEB J. 35 (6) https://doi.org/10.1096/FJ.202002766R.

Li, X.H., Xue, C., Liu, M.Q., et al., 2021b. Attractin gene deficiency in rats leads to impairments in both activity and spatial learning and memory. Neuroscience 466, 101–108. https://doi.org/10.1016/J.NEUROSCIENCE.2021.05.006.

Magid-Bernstein, J., Girard, R., Polster, S., et al., 2022. Cerebral hemorrhage: pathophysiology, treatment, and future directions. Circ. Res. 130 (8), 1204–1229. https://doi.org/10.1161/CIRCRESAHA.121.319949.

Martin, F., Malergue, F., Pitari, G., et al., 2001. Vanin genes are clustered (human 6q22-24 and mouse 10A2B1) and encode isoforms of pantetheinase ectoenzymes. Immunogenetics 53 (4), 296–306. https://doi.org/10.1007/S002510100327.

Moon, S.Y., Zheng, Y., 2003. Rho GTPase-activating proteins in cell regulation. Trends Cell Biol. 13 (1), 13–22. https://doi.org/10.1016/S0962-8924(02)00004-1.

Otero-Ortega, L., Alonso-López, E., Pérez-Mato, M., et al., 2021. Circulating extracellular vesicle proteins and MicroRNA profiles in subcortical and cortical-subcortical Ischaemic stroke. Biomedicines 9 (7). https://doi.org/10.3390/BIOMEDICINES9070786.

Pathak, A., Agrawal, A., 2019. Evolution of C-reactive protein. Front. Immunol. 10 (APR) https://doi.org/10.3389/FIMMU.2019.00943.

Poverennaya, E.V., Pyatnitskiy, M.A., Dolgalev, G.V., et al., 2023. Exploiting multi-Omics profiling and systems biology to investigate functions of TOMM34. Biology (Basel.) 12 (2). https://doi.org/10.3390/BIOLOGY12020198/S1.

R: The R Project for Statistical Computing. Accessed September 17. https://www.r-project.org/.

Rajeev Kumar, S., Sakthiswary, R., Lokanathan, Y., 2024. Potential therapeutic application and mechanism of action of stem cell-derived extracellular vesicles (EVs) in systemic lupus erythematosus (SLE). Int. J. Mol. Sci. 25 (4), 2444. https://doi.org/10.3390/IJMS25042444/S1.

Sack, G.H., 2018. Serum amyloid a - a review. Mol. Med. 24 (1) https://doi.org/10.1186/S10020-018-0047-0.

Salleron, L., Magistrelli, G., Mary, C., Fischer, N., Bairoch, A., Lane, L., 2014. DERA is the human deoxyribose phosphate aldolase and is involved in stress response. Biochim. Biophys. Acta 1843 (12), 2913–2925. https://doi.org/10.1016/J.BBAMCR.2014.09.007.

Sandset, E.C., Anderson, C.S., Bath, P.M., et al., 2021. European stroke organisation (ESO) guidelines on blood pressure management in acute ischaemic stroke and intracerebral haemorrhage. Eur. Stroke J. 6 (2) https://doi.org/10.1177/23969873211012133/ASSET/IMAGES/LARGE/10.1177_23969873211012133-FIG1.JPEG. XLVIII-LXXXIX.

Sawant, H., Bihl, T., Nguyen, D., Iwuchukwu, I., Bihl, J., 2022. The profile of inflammatory extracellular vesicles in intracerebral hemorrhage patients. Front. Stroke 1. https://doi.org/10.3389/fstro.2022.988081.

Shahrour, M.A., Ashhab, M., Edvardson, S., Gur, M., Abu-Libdeh, B., Elpeleg, O., 2017. Hypomyelinating leukodystrophy associated with a deleterious mutation in the ATRN gene. Neurogenetics 18 (3), 135–139. https://doi.org/10.1007/S10048-017-0515-7.

Shao, Z., Tu, S., Shao, A., 2019. Pathophysiological mechanisms and potential therapeutic targets in intracerebral hemorrhage. Front. Pharmacol. 10. https://doi.org/10.3389/FPHAR.2019.01079.

Tang, W., Duke-Cohan, J.S., 2002. Human secreted attractin disrupts neurite formation in differentiating cortical neural cells in vitro. J. Neuropathol. Exp. Neurol. 61 (9), 767–777. https://doi.org/10.1093/JNEN/61.9.767.

Théry, C., Witwer, K.W., Aikawa, E., et al., 2018. Minimal information for studies of extracellular vesicles 2018 (MISEV2018): a position statement of the International Society for Extracellular Vesicles and update of the MISEV2014 guidelines. J. Extracell Vesicles 7 (1). https://doi.org/10.1080/20013078.2018.1535750.

von Kügelgen, I., 2017. Structure, pharmacology and roles in physiology of the P2Y12 receptor. Adv. Exp. Med. Biol. 1051, 123–138. https://doi.org/10.1007/5584_2017_98.

Zhang, R., Xue, M., Yong, V.W., 2021. Central nervous system tissue regeneration after intracerebral hemorrhage: the next frontier. Cells 10 (10). https://doi.org/10.3390/CELLS10102513.

Zhang, W., Wu, Q., Hao, S., Chen, S., 2022. The hallmark and crosstalk of immune cells after intracerebral hemorrhage: immunotherapy perspectives. Front. Neurosci. 16 https://doi.org/10.3389/FNINS.2022.1117999.

Zou, Y., Liao, L., Dai, J., et al., 2023. Mesenchymal stem cell-derived extracellular vesicles/exosome: a promising therapeutic strategy for intracerebral hemorrhage. Regen Ther. 22, 181–190. https://doi.org/10.1016/J.RETH.2023.01.006.